Hindawi
Geofluids
Volume 2022, Article ID 9264959, 10 pages
https://doi.org/10.1155/2022/9264959

Research Article

The Layout of the Combustion Cavity and the Fracture Evolution of the Overlying Rock during the Process of Underground Coal Gasification

Zhaolin Li,[1,2] **Lianguo Wang**,[3] **Bo Ren**,[3] **and Ke Ding**[3]

[1]*School of Mines, China University of Mining and Technology, Xuzhou, Jiangsu 221116, China*
[2]*State Key Laboratory of Coal Resources and Safe Mining, China University of Mining and Technology, Xuzhou, Jiangsu 221116, China*
[3]*State Key Laboratory for Geomechanics and Deep Underground Engineering, China University of Mining and Technology, Xuzhou, Jiangsu 221116, China*

Correspondence should be addressed to Lianguo Wang; cumt_lgwang@163.com

Received 5 November 2021; Accepted 19 March 2022; Published 4 April 2022

Academic Editor: Fazhi Yan

Based on the thermodynamic and elastodynamic theories, the controlling equation of temperature-stress coupling action on rocks containing random damage units is established by combining the Mogi-Coulomb damage criterion. And the numerical calculation model of combustion cavity expansion under temperature-stress coupling condition is established by using ABAQUS secondary development program. The fracture field evolution law during the expansion of the gasification cavity was studied under two conditions: perpendicular to (condition 1) and along the intermediate principal stress (condition 2). It is found that under the condition 1, the gasification cavity gradually forms a smaller fracture circle, while the surrounding rock at the floor of the gasification cavity generates a wide range of equivalent damage areas under the condition 2, which is unfavorable for practical engineering. The condition 1 deployment scheme is more practical in terms of the degree of rupture and the subsequent gasification process. The gasification cavity is obviously affected by the horizontal stress. When the horizontal stress is small, the stability of the surrounding rock is seriously damaged. It is necessary to fully consider the influence of in situ stress in the layout of the gasification cavity; at the same time, measures are added to the process to reduce the degree of rupture of the surrounding rock. The evolution law of the temperature field and rupture field of the surrounding pressure in the combustion cavity during the whole process of UCG was numerically simulated. The floor rupture zone develops gradually with the advancement of the working face of the combustion cavity, and deeper rupture zones appear in several areas, which need special attention in the engineering.

1. Introduction

Underground coal gasification (UCG) is a new and environmentally friendly mining method [1], which can produce combustible gas mixture by controlled combustion of coal in situ underground under the action of a series of chemical reactions [2]. It is a mining method that integrates well construction, mining, and gasification, with the characteristics of green mining and clean utilization [3]. In the process of UCG, a key technology is how to effectively evaluate and control the stability of surrounding rocks in the combustion zone [4].

The rock temperature around the combustion cavity formed by UCG is as high as 700~1000° [5]. Under the action of high temperature [6], the surrounding rock of combustion cavity zone generates a large number of microcracks at the boundary of mineral particles due to thermal expansion [7], which seriously affects its stability [8]. Related studies on the evolution of rock fracture damage at high temperatures were also carried out by scholars such as Meng et al. [9], Fan et al. [10], and Ding et al. [11]. Therefore, how to effectively control the stability of the gasification cavity is a key technology in the process of UCG [12].

In essence, the destruction of surrounding rock caused by coal mining is a spatiotemporal evolutionary process [13]. Under the high temperature and in situ stress of coal bed gasification, the surrounding rock around the combustion cavity will form a fracture zone [14]. Once the rupture zone is connected to the underground aquifer, a water permeation accident will be triggered. At the same time, the gas in the gasification cavity may leak or overflow the ground, polluting the environment [15], which will cause the gasification cavity to fail to produce normally or even cause production shutdown accidents [16]. In addition, more serious is the connection between the rupture zone and the underground aquifer that may cause a large amount of groundwater leakage, which will cause great damage to the groundwater resources [17].

As the combustion cavity formed by UCG is often in a three-directional stress state [18], with the expansion of the combustion cavity area, the structural equilibrium of the surrounding rock is broken [19], resulting in the redistribution of the surrounding rock stress field [20]. The combustion cavity is often in a true triaxial stress state, with its stability closely related to the three-dimensional stress environment. Especially, the layout of the gasification cavity will determine the long-term operational stability in the subsequent gasification process. Under the high temperature of coal seam combustion and three-dimensional ground stress, the overlying rocks in the combustion cavity will form fracture zone [21]. When the fracture zone of overlying rocks is connected with the water-bearing layer in the upper part of the coal seam [22], it will cause the accident of water penetration in the roof [23]. At the same time, the gas in the gasification cavity may leak or even spill out of the ground, which may prevent the normal operation of the gasification cavity and even cause a production stoppage [24].

In addition, the research team found that the rock rupture characteristics [25] under the real triaxial stress environment are very different from those of the conventional triaxial [26]. Therefore, the rupture evolution characteristics of combustion cavities under the influence of different stresses are analyzed by combining the three-dimensional ground stress state characteristics [27]. It is of great significance to reveal the rupture mechanism of combustion cavity under the combined effect of high temperature and three-dimensional stress field. Meanwhile, it is important to propose a reasonable gasification cavity layout and construction scheme [28].

In view of this, a controlling equation of rock temperature-stress coupling [29] action is established in this manuscript based on thermodynamic and elastodynamic theories [30]. The numerical calculation model of the combustion cavity expansion under the temperature-stress coupling condition is established by using ABAQUS secondary development program. The law of fracture field evolution during the expansion of the combustion cavity is studied, the influence of different stress fields on the stability of the gasification cavity is analyzed, and a reasonable construction scheme is proposed.

2. UCG Numerical Modeling

A geometric three-dimensional model (Figure 1) was created in ABAQUS to represent the teardrop-shaped characteristics [31] of the combustion cavity under single combustion point conditions [32]. Prabu and Jayanti [33] and Yang et al. [14] found that the gasification cavity formed after combustion was roughly teardrop-shaped; so, this feature will be used for the gasification cavity in this study. The teardrop-shaped combustion cavity is simplified to consist of half a sphere (radius $o-y=o-z=15$ m) and half an ellipsoid (short axis $o-y=o-z=15$ m, long axis $o-x2=30$ m). According to the height relationship of the seam, the limit height of the combustion cavity is the full combustion thickness of the coal seam (15 m).

The numerical calculation model uses a rectangular body of 125 m × 105 m × 35 m, which is simplified to three rock layers: the roof strata, the coal strata, and the floor strata (Figure 1(a)). The boundary conditions of the model are set as follows: the bottom surface is constrained by vertical displacement; the height of the overlying rock layer of the model is 550 m, which is loaded on the upper boundary of the model in the form of a uniform load with a magnitude of 15 MPa (σ_1); the maximum and minimum horizontal stresses are 12 MPa and 7 MPa, respectively. Two combustion cavity working conditions are designed: condition 1, σ_2 perpendicular to the horizontal combustion direction; condition 2, σ_2 along the horizontal combustion direction. The initial temperature of each rock layer before combustion is 30°C. The temperature of the combustion cavity surface (representing the gasification surface) is raised to 1000°C after the start of gasification.

Natural rocks contain a large number of microdefects such as randomly distributed microfractures inside [34]. A numerical model of rock rupture evolution containing random damage distribution is developed using the secondary development subroutine USDFLD [35]. The total percentage of damage units is n, with basic mechanical parameters about 1/2 of the intact units [36]. In addition, considering the influence of temperature, according to the theory of elasticity, the solid equilibrium differential equation that can be expressed by displacement is [37]

$$Gu_{i,jj}+\frac{G}{1-2v}u_{j,ji}+3KaT+F_i=0(i,j=1,2,3), \quad (1)$$

where u_i is the displacement component, F_i is the body force component, a is the linear thermal expansion coefficient of the rock, T is the temperature field, which is determined by the heat conduction control equation, G and K are the rock damage shear modulus and bulk modulus, and v is Poisson's ratio.

According to the principle of heat balance, it is assumed that the specific heat C and thermal conductivity k of the rock are constants that do not change with temperature. Then the differential equation of rock heat conduction control can be expressed as [38]

$$pC\frac{\partial T}{\partial t}=k\left(\frac{\partial^2 T}{\partial x^2}+\frac{\partial^2 T}{\partial y^2}+\frac{\partial^2 T}{\partial z^2}\right)+Q. \quad (2)$$

In the formula, p is the density of the rock, C and k are

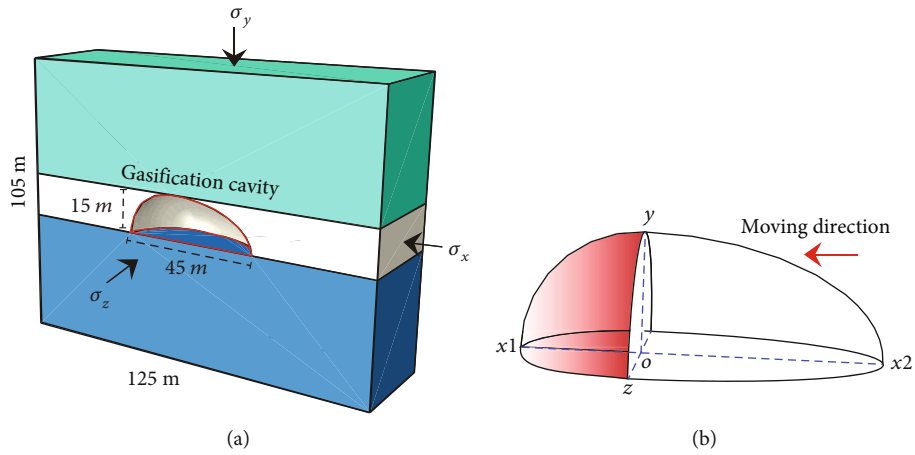

FIGURE 1: (a) Numerical calculation model. (b) Patterns of combustion cavity.

the specific heat capacity and thermal conductivity of the rock, and Q is the internal heat source of the rock.

Figure 2 shows the numerical calculation process. Since the Mogi-Coulomb strength criterion [39] is more suitable for the true triaxial ground stress environment [40], the strength criterion is used to determine whether the element is damaged [41]. The stiffness degradation of the rock failure unit is treated, and its stiffness is 1/10 of the original initial stiffness [42]. In order to facilitate the calculation, the rock layers are homogenized. The physical and mechanical parameters of each rock layer in the model are shown in Table 1.

Figure 3 shows the fracture characteristics of the surrounding rock of the gasification chamber under the two working conditions. The fracture zone characteristics are similar in both conditions, and the fracture circle is formed gradually near the surface of the gasification cavity. In addition, due to the arched structure of the gasification cavity roof, the fracture zone of the surrounding rock shifts to both sides, resulting in a relatively small fracture zone. Comparing the two working conditions, it can be found that the rupture zone is slightly larger in condition 2 (σ_2 along the horizontal combustion direction) than in condition 1.

Since the computational model uses the Mogi-Coulomb intensity criterion, its calculation equation [43] is

$$\tau_{oct} = a + b\sigma_{m,2},$$
$$\tau_{oct} = \frac{1}{3}\sqrt{(\sigma_1 - \sigma_2)^2 + (\sigma_2 - \sigma_3)^2 + (\sigma_1 - \sigma_3)^2}. \quad (3)$$

Among them, the magnitude of the equivalent effect force τ_{oct} has an important pointing significance in judging the rupture trend of the unit; so, the equivalent effect force τ_{oct} is used to quantify the rupture trend of the gasification cavity, as shown in Figure 4. The larger the equivalent force is, the more obvious the rupture trend is, and the higher equivalent force (over 10 MPa) is defined as the equivalent damage field in this paper.

Although there is little difference in the range of the rupture zone under the two working conditions, it can be found by comparing the two working conditions: in condition 1, the surrounding rock near the surface of the gasification cavity gradually forms a fracture circle, whose shape characteristics are roughly similar to those of the fracture zone, indicating that the damage characteristics of the surrounding rock can be better quantified by using equivalent forces. In addition, the "X" damage field was formed in the two arched shoulders and two bottom corners of the gasification cavity, which poses a potential risk for the continuation of the gasification process.

In condition 2, the surrounding rocks of the gasification cavity produced a wide range of equivalent damage zones, especially the surrounding rocks deep in the floor, which gradually converged with the far-field damage zone formed at the bottom boundary, forming a huge damage penetration zone. This is unfavorable for actual engineering. Once there is an aquifer in the bottom of the floor, it will cause the damage field to be connected to the aquifer, resulting in a substantial water-conducting rupture zone, which will cause a water penetration accident in the floor. The engineering can be avoided by reducing the height of the combustion cavity, the length of the combustion cavity direction, increasing the protection of coal pillars, and other ways to avoid the occurrence of water gushing accident at the bottom plate [44].

3. Horizontal Cross-Sectional Fracture Characteristics of the Combustion Cavity

For a single combustion point, the combustion cavity is approximately teardrop-shaped in the horizontal plane. Since the coal seam has no boundary in the horizontal direction, the combustion cavity expands along the horizontal direction until it reaches the designed combustion cavity width and finally forms a teardrop-shaped combustion cavity. In order to show more clearly the influence of stress field orientation on the rupture characteristics of the combustion cavity, a horizontal section combustion cavity model is established (Figure 5). Comparing the rupture evolution process of the combustion cavity under two working conditions, it can be found in the following:

In condition 1, the rupture zone is asymmetrically distributed near the front and rear ends of the gasification

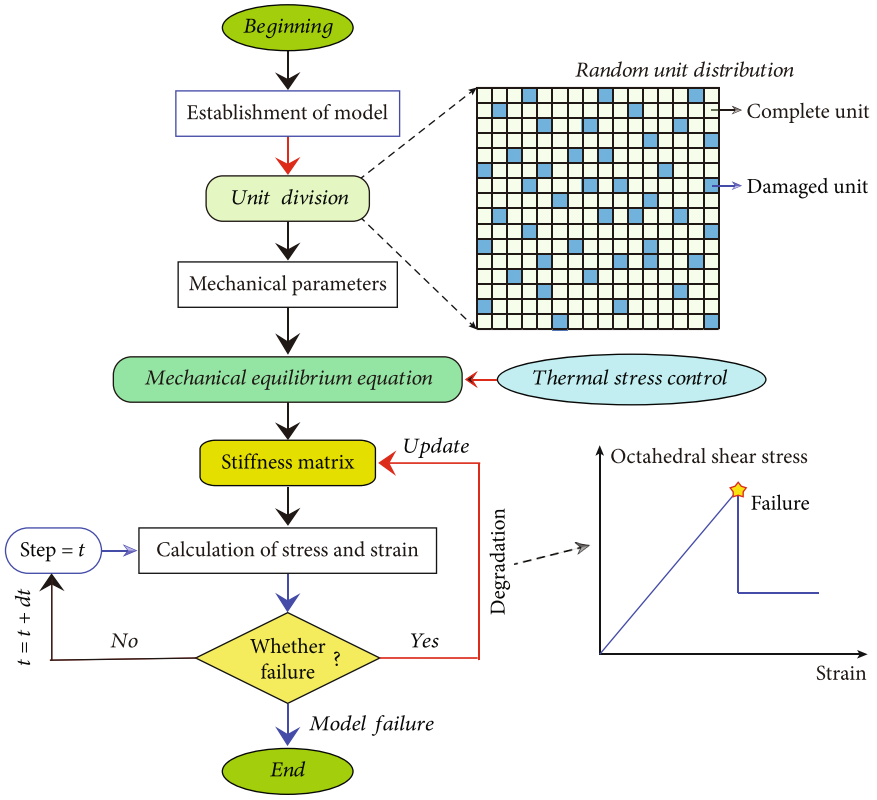

Figure 2: Flow chart of numerical simulation solution.

Table 1: Numerical model parameters.

Parameters	Roof strata	Coal strata	Floor strata
Young's modulus, E, GPa	16	10	18
Poisson's ratio, μ	0.3	0.33	0.3
Internal cohesion, c, MPa	3.5	2.5	3.6
Internal frictional angle, φ, °	35	26	37
The proportion of damaged elements, n_0, %	20%	30%	20%
Specific heat, C, J/(kg·°C)	890	1760	1650
Thermal conductivity, k, (J/h)/(kg·°C)	4320	1810	3240
Thermal expansion, α, (/°C)	2.3×10^{-6}	3.0×10^{-6}	2.4×10^{-6}

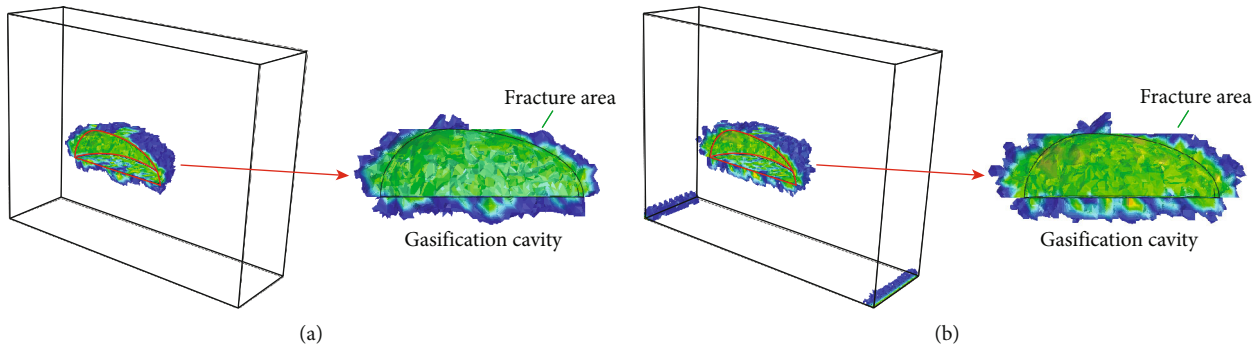

Figure 3: The fracture evolution law of surrounding rock in the combustion cavity: (a) condition 1 and (b) condition 2.

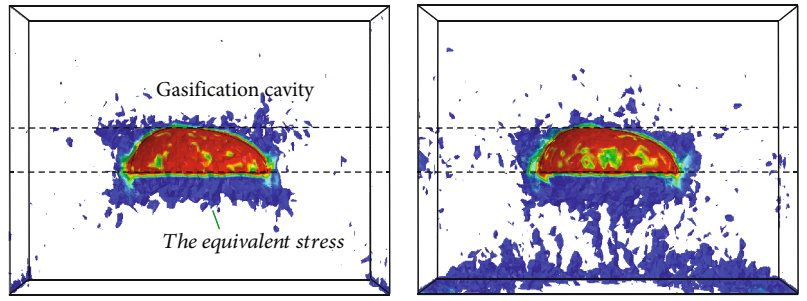

Figure 4: The variation pattern of the equivalent stress in the combustion cavity: (a) condition 1 and (b) condition 2.

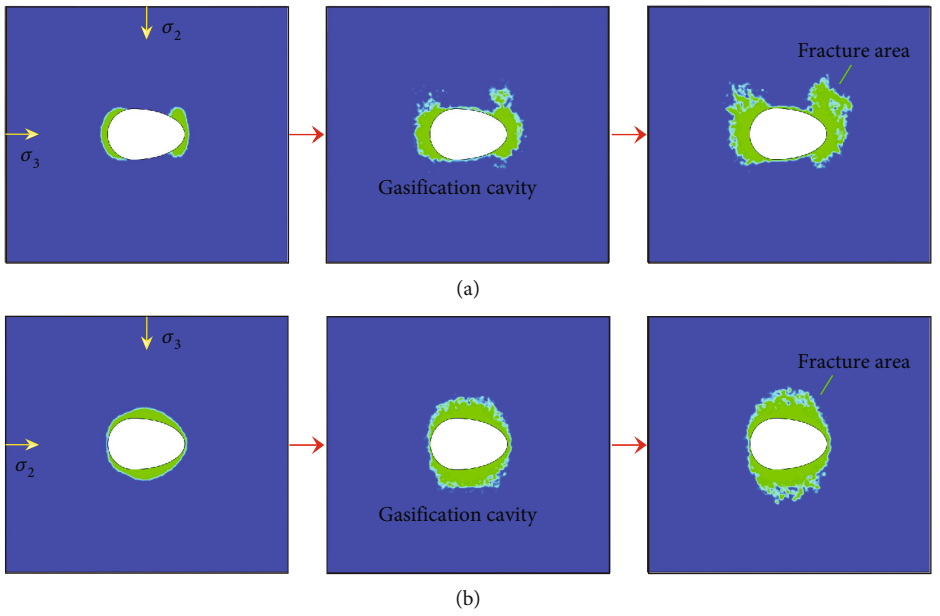

Figure 5: The influence of different principal stress orientations on the rupture characteristics of the combustion cavity: (a) condition (1) and (b) condition (2).

chamber owing to the fact that σ_2 is perpendicular to the horizontal combustion direction and the asymmetric circular shape of the combustion cavity boundary. As the gasification process proceeds, the rupture zone gradually expands. Since the gasification cavity will continue to retreat in the axial direction of the gasification channel after reaching the combustion boundary, the operating condition can be regarded as an advanced precracking of the surrounding rock of the gasification cavity in the next stage. As long as the fracture range of the coal seams on both sides is effectively controlled, the stability requirements of the surrounding rock of the gasification cavity can be met.

In condition 2, the rupture zone is symmetrically distributed due to σ^2 along the horizontal combustion direction, mainly concentrated in both sides of the gasification cavity (coal seam). Although the extent of the rupture zone is slightly reduced in this condition compared to condition one, the extent of rupture at the front and rear ends of the gasification cavity is extremely small. There is basically no impact on the next stage of gasification process, which is a waste from the perspective of energy utilization. Of course,

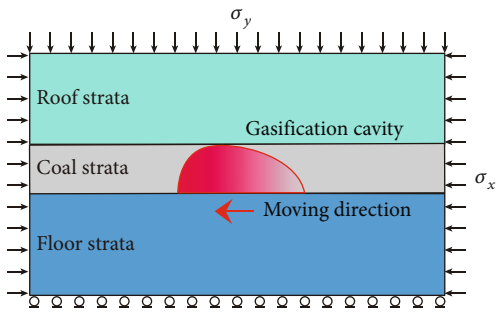

Figure 6: Numerical calculation model.

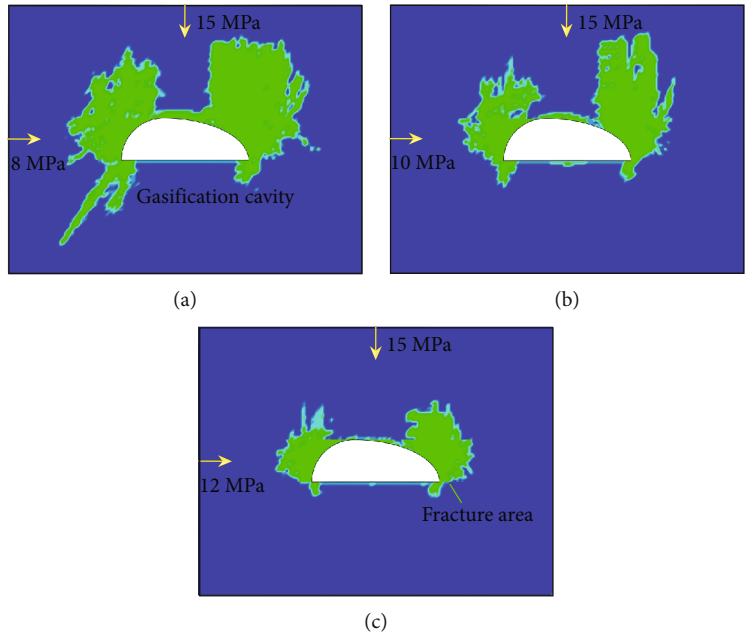

Figure 7: Effect of horizontal stress on the fracture area of the gasification cavity.

it is more advantageous for some projects to use a separate gasification chamber scheme (with lower recovery rate).

4. Fracture Characteristics of the Gasification Cavity in Axial Vertical Section

In order to analyze the influence of different stress states on the fracture characteristics in the axial and vertical section of the gasification cavity, the influence of the horizontal lateral stress on the gasification cavity was studied, and the vertical calculation model shown in Figure 6 was established. The boundary conditions are basically the same as those in Figure 1, where the vertical stress is constant at 15 MPa and the different horizontal stress magnitudes (8,10,12 MPa) are mainly changed. The basic dimensions of the gasification cavity and the physical and mechanical parameters of each rock layer are consistent with Table 1.

Figure 7 shows the effect of different horizontal stresses on the rupture zone of the gasification cavity. When the horizontal stress was small, a wide range of rupture zones appeared near the roof and two bottom corners of the combustion cavity. The stability of the surrounding rock all suffered serious damage, which will have an extremely negative impact on the continued advance of gasification afterwards. With the increase of horizontal stress, this phenomenon is alleviated, especially when the horizontal stress reaches 12 MPa, and the rupture zone of surrounding rock near the combustion cavity is greatly reduced. It shows that the influence of ground stress needs to be fully considered when the gasification chamber is arranged. When the horizontal stress is significantly lower than the vertical stress, a large-scale fracture zone will appear in the surrounding rock near the gasification cavity; so, special attention is needed in the process.

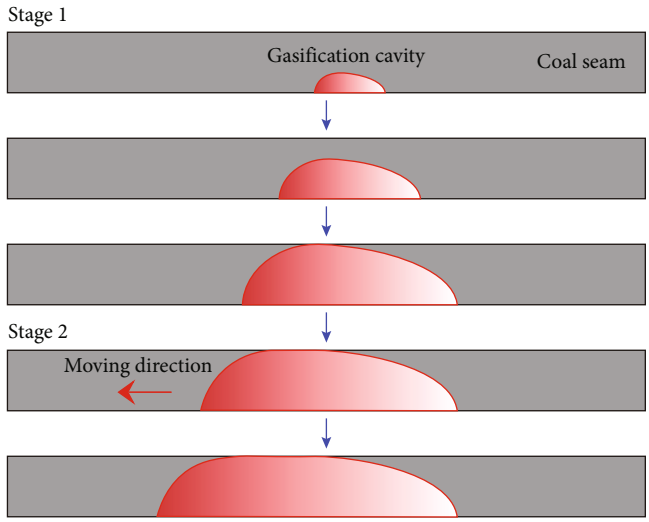

Figure 8: Two-stage development process of combustion cavity.

Based on the above analysis results, the stress distribution characteristics of working condition 2 are used to simulate more realistically the development pattern of gasification cavity in the whole process of UCG. In the numerical simulation design, the gasification cavity development is divided into 2 stages according to the thermoelastic instantonal equation and the temperature field control equation (Figure 2). In stage 1, the gasification cavity is small in size and expands equidistantly along the width and height directions in the coal seam until the top of the gasification cavity develops to the roof of the coal seam (1 m/d). The high-temperature gasification surface is gradually transferred to the downstream cavity wall of the gasification cavity in this stage. In stage 2, the gasification

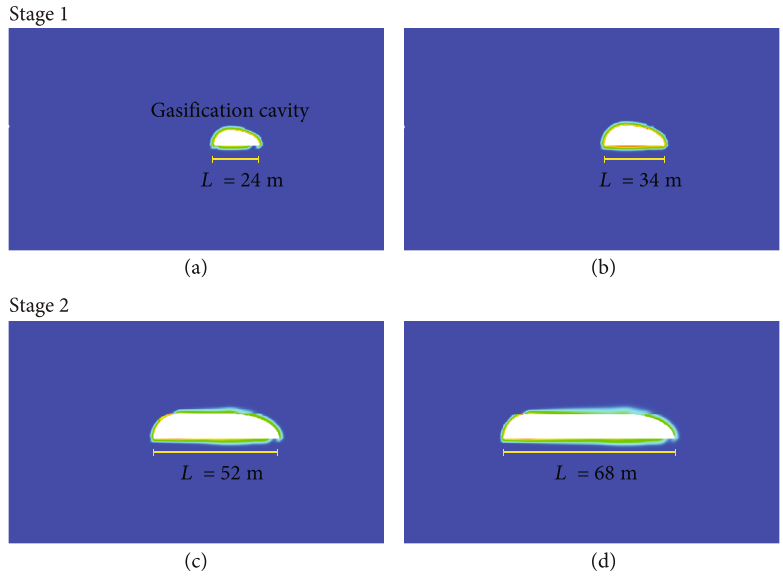

Figure 9: Temperature distribution characteristics of combustion cavity in stage1 and stage 2, respectively.

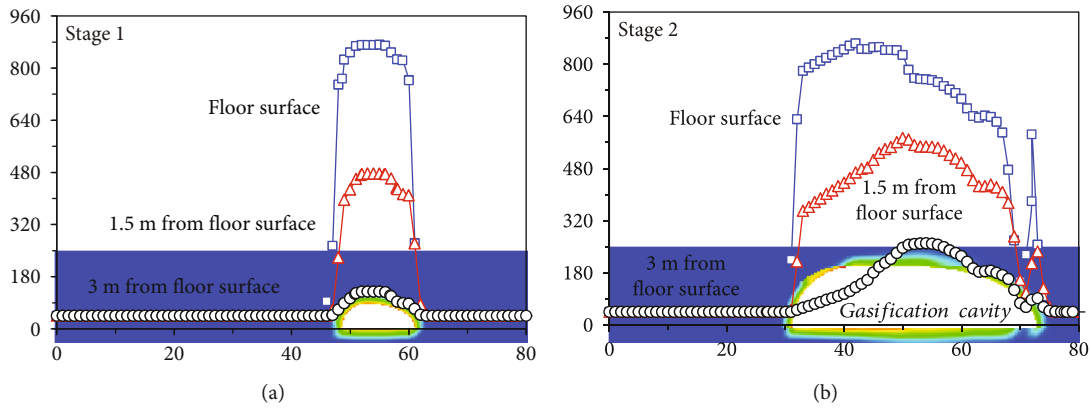

Figure 10: Temperature variation patterns at different depths of the coal seam floor: (a) stage 1 and (b) stage 2.

working surface is advanced horizontally and uniformly at a constant rate (1 m/d), with a constant height of the gasification chamber.

5. Characteristics of Surrounding Rock Temperature and Rupture Field in the Whole Process of UCG

Based on the above analysis results, the stress distribution characteristics of condition 2 are used to more truly simulate the development law of gasification chamber in the whole process of UCG. In the numerical simulation design, the gasification cavity development is divided into 2 stages according to the thermoelastic instantonal equation and the temperature field control equation (Figure 8). In stage 1, the gasification cavity is small in size and expands equidistantly along the width and height directions in the coal seam until the top of the gasification cavity develops to the roof of the coal seam (1 m/d). The high-temperature gasification surface is gradually transferred to the downstream cavity wall of the gasification cavity in this stage. In stage 2, the gasification working surface is advanced horizontally and uniformly at a constant rate (1 m/d), with a constant height of the gasification chamber.

Figure 9 shows the characteristics of the temperature field distribution around the combustion cavity during the combustion of the coal seam. In stage 1, the space of the combustion cavity is small, and the temperature on the surface of the coal wall and the roof and floor is basically the same, roughly around 950°C. With the burning of the coal wall, the combustion cavity enters stage 2 and advances to the left, with the space gradually increasing. The temperature of the surface of the combustion coal wall basically remains around 950°C during this process, and the temperature of the downstream of the gasification cavity wall gradually decreases, and when the

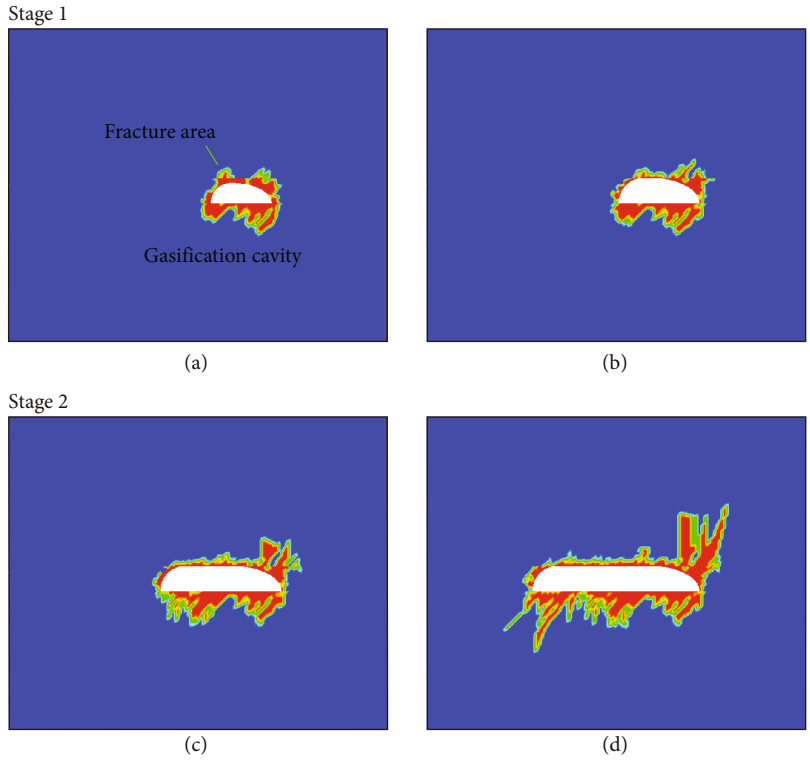

Figure 11: The evolution law of the failure characteristics around the surrounding rock of the combustion cavity.

length is 68 m, the temperature of the floor surface downstream has been reduced to around 350°C.

Figure 10 demonstrates the change pattern of temperature of the surrounding rock at different depths of the floor of the coal seam with the UCG process. The temperature on the surface of the floor upstream from the combustion cavity is basically about 950°C, with more drastic temperature changes. With the increase of the vertical distance from the coal seam, the temperature of the rock seam decreases rapidly. For example, the surrounding rock is about 1.5 m away from the floor surface, the temperature field changes gradually, and its maximum peak temperature is roughly half of the floor surface. The temperature field of surrounding rock 3 m from the floor surface has little influence, and the peak temperature is only about 210°C.

Figure 11 shows the evolution of the failure characteristics of the surrounding rock of the combustion cavity during the whole UCG process. In stage 1, the roof of the combustion cavity as well as the two bottom corners generated a wide range of rupture zones, especially the damage of the bottom plate was more obvious. Later, as the gasification process continued, it entered stage 2. A deeper rupture zone appeared near the initial arch on the right side of the gasification cavity, which was prone to roof collapse. The rupture zone of the floor is gradually developed with the advancement of the burning cavity working face, and deeper rupture zones appear in several areas, which need special attention in the engineering to avoid further increase of the rupture zone by leaving coal pillars and other means if necessary.

6. Conclusion

(1) Based on the thermodynamic and elastodynamic theories, the controlling equation of temperature-stress coupling action on rocks containing random damage units is established by combining the Mogi-Coulomb damage criterion. And the numerical calculation model of combustion cavity expansion under temperature-stress coupling condition is established by using ABAQUS secondary development program

(2) The fracture field evolution law during the expansion of the gasification cavity was studied under two conditions: perpendicular to (condition 1) and along the intermediate principal stress (condition 2). It is found that under the condition 1, the surrounding rock near the surface of the gasification cavity gradually forms a smaller fracture circle and an "X" type damage field appears; under the condition 2, the surrounding rock at the floor of the gasification cavity generates a wide range of equivalent damage areas, which is unfavorable for practical engineering

(3) The rupture characteristics of the horizontal section of the gasification chamber under the two working conditions were compared. It is found that the fracture areas of condition 1 are asymmetrically distributed near the front and end of the gasification cavity. In condition 2, the fracture areas are symmetrically

distributed and mainly concentrated in the horizontal sides of the gasification cavity. The condition 1 deployment scheme is more practical in terms of the degree of rupture and the subsequent gasification process

(4) The gasification cavity is obviously affected by the horizontal stress. When the horizontal stress is small, the stability of the surrounding rock is seriously damaged; with the increase of horizontal stress, the range of the surrounding rock fracture area is greatly reduced. It is necessary to fully consider the influence of in situ stress in the layout of the gasification cavity; at the same time, measures are added to the process to reduce the degree of rupture of the surrounding rock

(5) The evolution law of the temperature field and rupture field of the surrounding pressure in the combustion cavity during the whole process of UCG was numerically simulated. The upstream temperature of the gasification cavity shows an increasing trend, and the downstream temperature gradually decreases. A deeper rupture cavity appears near the initial vault on the right side of the gasification cavity, which is prone to roof collapse. The floor rupture zone develops gradually with the advancement of the working face of the combustion cavity, and deeper rupture zones appear in several areas, which need special attention in the engineering

Data Availability

The data used to support the findings of this study are available from the corresponding author upon request.

Conflicts of Interest

The authors declare that there are no conflicts of interest regarding the publication of this paper.

Acknowledgments

We gratefully acknowledge the support provided by Natural Science Foundation of Jiangsu Province, China (Grant No. BK20200628), China Postdoctoral Science Foundation Funded Project (Grant No. 2020M671649), and the Fundamental Research Funds for the Central Universities (Grant No. 2020QN42).

References

[1] H. Li, J. Zha, G. Guo, H. Zhang, Y. Xu, and Y. Niu, "Evaluation method of surface subsidence degree for underground coal gasification without shaft," *Combustion Science and Technology*, vol. 194, no. 3, pp. 608–621, 2022.

[2] R. Zagorščak, S. Sadasivam, H. R. Thomas, K. Stańczyk, and K. Kapusta, "Experimental study of underground coal gasification (UCG) of a high-rank coal using atmospheric and high-pressure conditions in an ex-situ reactor," *Fuel*, vol. 270, p. 117490, 2020.

[3] J. Wang, Z. Zu, Z. Wang, and G. Xu, "The design of ignition systems and a study of the development of the high temperature zone in well-type underground coal gasification," *Fuel*, vol. 269, p. 117281, 2020.

[4] P. Hou, X. Liang, F. Gao, J. Dong, J. He, and Y. Xue, "Quantitative visualization and characteristics of gas flow in 3D pore-fracture system of tight rock based on lattice Boltzmann simulation," *Journal of Natural Gas Science and Engineering*, vol. 89, p. 103867, 2021.

[5] L. Xin, C. Li, W. Liu et al., "Change of sandstone microstructure and mineral transformation nearby UCG channel," *Fuel Processing Technology*, vol. 211, p. 106575, 2021.

[6] Z. Liu, M. Zhang, S. Yu, L. Xin, G. Wang, and L. Sun, "Experimental study on the fractal features and permeability characteristics of low metamorphic coal pore structure under thermal damage," *Geofluids*, vol. 2020, Article ID 8864571, 13 pages, 2020.

[7] J. Li, Z.-W. Du, and Z.-P. Guo, "Effect of high temperature (600°C) on mechanical properties, mineral composition, and microfracture characteristics of sandstone," *Advances in Materials Science and Engineering*, vol. 2020, Article ID 5072534, 19 pages, 2020.

[8] W. Huang and Z. Wang, "Mechanical performance evolution and size determination of strip coal pillars with an account of thermo-mechanical coupling in underground coal gasification," *International Journal of Rock Mechanics and Mining Sciences*, vol. 142, p. 104755, 2021.

[9] T. Meng, X. Guangwu, M. Jiwei et al., "Mixed mode fracture tests and inversion of FPZ at crack tip of overlying strata in underground coal gasification combustion cavity under real-time high temperature condition," *Engineering Fracture Mechanics*, vol. 239, p. 107298, 2020.

[10] L. F. Fan, J. W. Gao, Z. J. Wu, S. Q. Yang, and G. W. Ma, "An investigation of thermal effects on micro-properties of granite by X-ray CT technique," *Applied Thermal Engineering*, vol. 140, pp. 505–519, 2018.

[11] K. Ding, L. Wang, B. Ren, Z. Li, S. Wang, and C. Jiang, "Experimental study on relative permeability characteristics for CO2 in sandstone under high temperature and overburden pressure," *Minerals*, vol. 11, no. 9, p. 956, 2021.

[12] R. Mandal, T. Maity, S. K. Chaulya, and G. M. Prasad, "Laboratory investigation on underground coal gasification technique with real- time analysis," *Fuel*, vol. 275, p. 117865, 2020.

[13] P. Hou, X. Liang, Y. Zhang, J. He, F. Gao, and J. Liu, "3D multi-scale reconstruction of fractured shale and influence of fracture morphology on shale gas flow," *Natural Resources Research*, vol. 30, no. 3, pp. 2463–2481, 2021.

[14] D. Yang, N. Koukouzas, M. Green, and Y. Sheng, "Recent development on underground coal gasification and subsequent CO_2 storage," *Journal of the Energy Institute*, vol. 89, no. 4, pp. 469–484, 2016.

[15] X. Liang, P. Hou, Y. Xue, X. Yang, F. Gao, and J. Liu, "A fractal perspective on fracture initiation and propagation of reservoir rocks under water and nitrogen fracturing," *Fractals*, vol. 29, no. 7, p. 2150189, 2021.

[16] C. Otto, T. Kempka, K. Kapusta, and K. Stańczyk, "Fault reactivation can generate hydraulic short circuits in underground coal gasification—new insights from regional-scale thermo-mechanical 3D modeling," *Minerals*, vol. 6, no. 4, p. 101, 2016.

[17] K. Zhao, N. Xu, G. Mei, and H. Tian, "Predicting the distribution of ground fissures and water-conducted fissures induced

by coal mining: a case study," *SpringerPlus*, vol. 5, no. 1, p. 977, 2016.

[18] W. Xiao, D. Zhang, H. Li, G. Yu, H. Yang, and B. Yu, "Difference analysis on sandstone permeability after treatment at different temperatures during the failure process: a case study of sandstone in Chongqing, China," *Pure and Applied Geophysics*, vol. 178, no. 5, pp. 1893–1910, 2021.

[19] B. Mahanta, P. G. Ranjith, V. Vishal, and T. N. Singh, "Temperature-induced deformational responses and microstructural alteration of sandstone," *Journal of Petroleum Science and Engineering*, vol. 192, p. 107239, 2020.

[20] W. Gao, R. Zagorščak, and H. R. Thomas, "Insights into solid-gas conversion and cavity growth during underground coal gasification (UCG) through thermo-hydraulic-chemical (THC) modelling," *International Journal of Coal Geology*, vol. 237, p. 103711, 2021.

[21] S. Daggupati, R. N. Mandapati, S. M. Mahajani et al., "Compartment modeling and flow characterization in nonisothermal underground coal gasification cavities," *Industrial & Engineering Chemistry Research*, vol. 51, no. 12, pp. 4493–4508, 2012.

[22] L. Xin, J. Li, J. Xie, C. Li, and Z. Wang, "Simulation of cavity extension formation in the early ignition stage based on a coal block gasification experiment," *Journal of Energy Resources Technology*, vol. 142, no. 6, pp. 1–12, 2019.

[23] X. Liu, G. Guo, and H. Li, "Study on the propagation law of temperature field in surrounding rock of underground coal gasification (UCG) combustion cavity based on dynamic thermal parameters," *Results in Physics*, vol. 12, pp. 1956–1963, 2019.

[24] S. Daggupati, R. N. Mandapati, S. M. Mahajani et al., "Laboratory studies on cavity growth and product gas composition in the context of underground coal gasification," *Energy*, vol. 36, no. 3, pp. 1776–1784, 2011.

[25] Z. Li, L. Wang, Y. Lu, W. Li, and K. Wang, "Experimental investigation on the deformation, strength, and acoustic emission characteristics of sandstone under true triaxial compression," *Advances in Materials Science and Engineering*, vol. 2018, Article ID 5241386, 16 pages, 2018.

[26] Z. Li, L. Wang, Y. Lu, W. Li, K. Wang, and H. Fan, "Experimental investigation on true triaxial deformation and progressive damage behaviour of sandstone," *Scientific Reports*, vol. 9, no. 1, pp. 442–455, 2019.

[27] X. Zha, H. Wang, and S. Cheng, "Finite element analysis of the subsidence of cap rocks during underground coal gasification process," in *Advanced Materials Research*, vol. 859, pp. 91–94, Trans Tech Publications Ltd, 2014.

[28] S. B. Javed, A. A. Uppal, A. I. Bhatti, and R. Samar, "Prediction and parametric analysis of cavity growth for the underground coal gasification project Thar," *Energy*, vol. 172, pp. 1277–1290, 2019.

[29] S. Vidana Pathiranagei, I. Gratchev, and R. Kong, "Engineering properties of four different rocks after heat treatment," *Geomechanics and Geophysics for Geo-Energy and Geo-Resources*, vol. 7, no. 1, pp. 1–21, 2021.

[30] R. Pakzad, S. Y. Wang, and S. W. Sloan, "Numerical simulation of hydraulic fracturing in low-/high-permeability, quasi-brittle and heterogeneous rocks," *Rock Mechanics and Rock Engineering*, vol. 51, no. 4, pp. 1153–1171, 2018.

[31] A. Jowkar, F. Sereshki, and M. Najafi, "A new model for evaluation of cavity shape and volume during underground coal gasification process," *Energy*, vol. 148, pp. 756–765, 2018.

[32] G. Samdani, P. Aghalayam, A. Ganesh, R. K. Sapru, B. L. Lohar, and S. Mahajani, "A process model for underground coal gasification - Part-I: cavity growth," *Fuel*, vol. 181, pp. 690–703, 2016.

[33] V. Prabu and S. Jayanti, "Simulation of cavity formation in underground coal gasification using bore hole combustion experiments," *Energy*, vol. 36, no. 10, pp. 5854–5864, 2011.

[34] P. Hou, S. Su, X. Liang et al., "Effect of liquid nitrogen freeze-thaw cycle on fracture toughness and energy release rate of saturated sandstone," *Engineering Fracture Mechanics*, vol. 258, p. 108066, 2021.

[35] S. Wang, Z. Li, R. Yuan, G. Li, and D. Li, "A shear hardening model for cohesive element method and its application in modeling shear hydraulic fractures in fractured reservoirs," *Journal of Natural Gas Science and Engineering*, vol. 83, p. 103580, 2020.

[36] W. Li, B. Jiang, S. Gu, X. Yang, and F. U. A. Shaikh, "Experimental study on the shear behaviour of grout-infilled specimens and micromechanical properties of grout-rock interface," *Journal of Central South University*, vol. 29, pp. 1–14, 2022.

[37] T. H. Duan, J. M. Zhang, C. Mallett, H. H. Li, L. W. Huo, and K. T. Zhao, "Numerical simulation of coupled thermal-mechanical fracturing in underground coal gasification," *Proceedings of the Institution of Mechanical Engineers Part a-Journal of Power and Energy*, vol. 232, no. 1, pp. 74–84, 2018.

[38] X. Wu, Q. Guo, P. Li, F. Ren, J. Zhang, and M. Cai, "Investigating the effect of temperature changes on the physical field of surrounding rock in a deep gold mine," *Advances in Materials Science and Engineering*, vol. 2021, Article ID 8490864, 13 pages, 2021.

[39] S. Aditya, K. S. Rao, and R. Ayothiraman, "An analytical solution to wellbore stability using Mogi-Coulomb failure criterion," *Journal of Rock Mechanics and Geotechnical Engineering*, vol. 11, no. 6, pp. 1211–1230, 2019.

[40] F. Feng, X. Li, J. Rostami, D. Peng, D. Li, and K. Du, "Numerical investigation of hard rock strength and fracturing under polyaxial compression based on Mogi-Coulomb failure criterion," *International Journal of Geomechanics*, vol. 19, no. 4, p. 04019005, 2019.

[41] Q. Feng, J. Jin, S. Zhang, W. Liu, X. Yang, and W. Li, "Study on a damage model and uniaxial compression simulation method of frozen–thawed rock," *Rock Mechanics and Rock Engineering*, vol. 55, no. 1, pp. 187–211, 2022.

[42] T. Li, L. Li, C. Tang et al., "A coupled hydraulic-mechanical-damage geotechnical model for simulation of fracture propagation in geological media during hydraulic fracturing," *Journal of Petroleum Science and Engineering*, vol. 173, pp. 1390–1416, 2019.

[43] Z. Song, G. Yin, P. G. Ranjith, M. Li, J. Huang, and C. Liu, "Influence of the intermediate principal stress on sandstone failure," *Rock Mechanics and Rock Engineering*, vol. 52, no. 9, pp. 3033–3046, 2019.

[44] G. Wałowski, "Gas permeability model for porous materials from underground coal gasification technology," *Energies*, vol. 14, no. 15, p. 4462, 2021.